

Aerosol-induced air breakdown with CO₂ laser radiation

David C. Smith and Robert T. Brown

Citation: [Journal of Applied Physics](#) **46**, 1146 (1975); doi: 10.1063/1.322215

View online: <http://dx.doi.org/10.1063/1.322215>

View Table of Contents: <http://scitation.aip.org/content/aip/journal/jap/46/3?ver=pdfcov>

Published by the [AIP Publishing](#)

Articles you may be interested in

[Aerosol-induced cumulus congestus moistening of the atmosphere](#)

AIP Conf. Proc. **1527**, 774 (2013); 10.1063/1.4803386

[Study of electrical breakdown induced by pulsed CO₂ laser radiation](#)

J. Appl. Phys. **59**, 1904 (1986); 10.1063/1.336418

[Two-dimensional modeling of aerosol-induced breakdown in air](#)

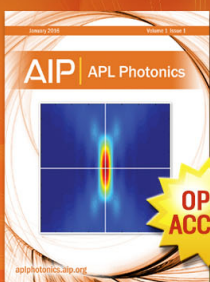
J. Appl. Phys. **50**, 4307 (1979); 10.1063/1.326467

[Aerosol-induced thermal blooming](#)

J. Appl. Phys. **46**, 402 (1975); 10.1063/1.321350

[Intracavity Radiation-Induced Air Breakdown in a TEA CO₂ Laser](#)

Appl. Phys. Lett. **19**, 433 (1971); 10.1063/1.1653760



Launching in 2016!

The future of applied photonics research is here

AIP | APL
Photonics

Aerosol-induced air breakdown with CO₂ laser radiation

David C. Smith and Robert T. Brown

United Aircraft Corporation, East Hartford, Connecticut 06108

(Received 16 September 1974)

The breakdown threshold with 10.6- μ wavelength CO₂ laser radiation induced by particles is reported. Single solid particles of different materials and sizes were suspended electrostatically at the focus of a pulsed TEA laser and the thresholds for vaporization and also for particle-induced breakdown were measured. The threshold intensity for breakdown is of the order 10⁸ W/cm², independent of particle size and material and represents the limiting intensity that can be propagated through an aerosol-laden atmosphere.

I. INTRODUCTION

Gas breakdown and plasma heating with laser radiation have been studied extensively for many years. One aspect of gas breakdown of particular importance concerns the power density which can be transmitted through a gas. When breakdown occurs the plasma produced is highly conducting and absorbs almost all of the subsequent laser radiation incident on the plasma. For visible and near-infrared laser radiation it was shown theoretically by Raizer¹ that the classical theory of microwave absorption could be used to predict the threshold intensities for gas breakdown. For small laser focal spots, the thresholds measured experimentally with ruby (0.69- μ wavelength) and neodymium (1.06- μ) laser radiation^{2,3} agreed well with those predicted by the classical microwave theory.⁴

However it was observed that the threshold for breakdown decreased inversely with focal spot diameter,² contrary to that predicted by any theoretical model.⁵ Several possible explanations were offered,^{6,7} but no satisfactory theory explained the experimental results. With the advent of the CO₂ laser, a number of experiments were conducted to determine the threshold intensity for breakdown with 10.6- μ wavelength radiation.⁸ Again, for small focal spots, the threshold agreed well with that predicted by microwave theory; i.e., the threshold intensity decreased as the wavelength squared.⁸ For visible laser radiation the breakdown threshold was observed to increase with wavelength, an unexplained result.⁹

Even for the 10.6- μ wavelength it was again shown that the threshold decreased inversely with laser beam diameter.¹⁰ This focal diameter dependence made scaling of the experimental results difficult if not impossible and showed thresholds that were nearly 2 orders of magnitude lower than those predicted by theoretical models.¹¹ An explanation of the diameter dependence which involved the interaction of the laser radiation with particulate matter suspended in air was proposed by Canavan and Nielsen.¹² Their proposed explanation related the inverse focal diameter dependence of the threshold to the probability of a particle of a certain size being in the focal volume, taking into account the distribution of particles as a function of particle radius. Lencioni¹³ verified that in the absence of particles the threshold of clean air agreed quantitatively with that predicted by the classical microwave theory. This was substantiated by Smith *et al.*¹⁴ for even larger focal spot diameters, and also by Brown and Smith¹⁵ for break-

down in preionized helium. The influence of aerosols on breakdown had therefore been shown to be of more importance as an atmospheric propagation limit than the limit associated with clean gas breakdown, since the threshold for particle-induced gas breakdown was substantially lower. Aerosols are almost always present in both the atmosphere and laboratory air and are extremely difficult to eliminate over long paths. In fact, the breakdown thresholds of gases in closed cells of high initial purity were found to have the same dependence on focal spot diameter as that associated with laboratory air,^{2,10} and this result is now attributed to particles driven from the cell walls when irradiated with the high-power beam and broken down with subsequent pulses.

Because of this importance for atmospheric propagation, a detailed experimental study was undertaken to examine the interaction of particulate matter with high-power pulsed CO₂ laser radiation. In order to study the details of the interaction, an electrodynamic suspension system was used to suspend a single particle at the focus of a lens, which allowed study of the interaction without interference from particle-supporting structures or interference by other particles in the vicinity of the target particle. The particle-induced air breakdown threshold with pulsed CO₂ laser radiation was studied as a function of particle material, particle size, and background air pressure. Schlieren and streak photography were used to examine the plasma growth. A qualitative theoretical model is suggested which is consistent with the experimental results. Comparison of previous results obtained at 1.06 μ with the present 10.6- μ data enables us to predict the wavelength dependence of aerosol-induced breakdown.

II. EXPERIMENTAL APPARATUS AND DATA

The previous studies of laser interaction with aerosols leading to gas breakdown involved the use of particle clouds, particles dropped through the focus of the laser, or particles attached to fine wires. These techniques for introducing the particles made the experiments difficult to operate and led to uncertainties in the interpretation of the data. Unique to the studies presented here is the particle suspension apparatus in which a single particle of chosen size and composition could be positioned at the focus of a high-power laser.

The laser used in the experiments was an atmospheric pressure electrically pulsed CO₂ laser with an output wavelength of 10.6 μ .¹⁶ The laser consisted of a 3-m-

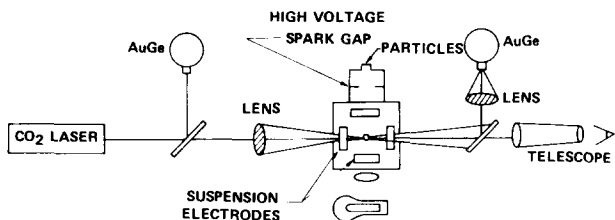


FIG. 1. Diagram of aerosol-induced breakdown experiment.

long by 5-cm-diam acrylic tube with a series of in-line electrodes. This laser produced a reproducible laser pulse with an energy of approximately 1 J and with a laser pulse shape consisting of an initial spike of 0.2- μ sec full width at half-maximum followed by a lower-intensity tail which lasted for 1–2 μ sec. Approximately one-third of the energy of the pulse was in the leading spike. This laser produced the pulse just described when it was operated with a gas mixture of CO₂, N₂, and He, or it could be operated without the nitrogen, in which case it produced a pulse of 0.2- μ sec duration without the low-intensity tail. This was a particularly attractive feature of this laser and was useful in determining whether the threshold for vaporization of particles depended on the peak intensity or on the energy content of the pulse by comparing thresholds with the two different pulse shapes. The laser had a divergence of 4×10^{-3} rad full angle corresponding to the half-power points of the focused laser beam. The laser pulse had some temporal and spatial structure, which affected the absolute magnitude of the measurements somewhat, but had only a small effect on the relative values. The intensity of the laser was varied by inserting partially reflecting germanium flats into the beam, allowing the laser intensity to be varied without changing the beam characteristics.

A. Particle suspension apparatus

The particle suspension apparatus consisted of a cubical array of electrodes which were connected to a three-phase ac power supply. The suspension system was similar to the one described in Ref. 17 and used in Ref. 18 for laser-plasma interaction studies, with the exception that the present system was operated at atmospheric pressure. Each pair of opposite electrodes was connected to one phase of the ac supply and had a variable voltage of up to 3 kV. The electrodes also had a variable dc bias of up to 300 V which was used for positioning the particle at the focus of the lens. The cube was approximately a 6.2-cm square and the electrodes were 5-cm diam copper disks with 2.5-cm-diam holes. The holes allowed the entrance of the laser beam, transmission measurements, illumination of the particles with a 300-W projector lamp, as well as visual observation of the laser-particle interaction. In order to suspend the particles in the cube, it was necessary to charge them electrically. In the previous suspension system^{17,18} the particles were suspended in vacuum and were charged with a heated filament electron gun; however, this technique could not be used with our system. Instead, the particles were placed in a container above the cube and dropped through an electrical discharge

powered by a simple Tesla coil, picking up sufficient charge to be suspended in the cube. The particles followed an elliptical orbit which was minimized by positioning the particle with the dc bias. In general the elliptical orbit had a diameter of roughly three times the 50- μ particle diameter.

A schematic of the experimental apparatus is shown in Fig. 1. The particles to be used in the experiment were preselected, sized, and placed in the column above the cube. The vibration from the Tesla spark discharge was sufficient to cause a few particles to fall through a small pinhole. There existed a position in the cube where the particle orbit had a minimum size and was most stable. The lens focus was located in the center of the cube by positioning a fine wire at the focus and maximizing the plasma produced by the laser interaction with the wire. The cross hairs of the two telescopes were then aligned on this spot and the wire was removed. The particle was located in its minimum orbit and the entire cube was then translated until the minimum orbit was centered on the cross hairs of the telescope by varying the dc bias on the electrodes. In these experiments, the focal spot size was 500 μ and the maximum particle size was 70 μ , so that alignment was not extremely critical.

The transmission of laser radiation through the focus was measured by focusing the beam exiting the cube onto a gold-doped germanium detector as shown in Fig. 1. The reflector shown at 45° was uncoated glass which was partially reflecting at the 10.6- μ CO₂ laser wavelength but was transmitting in the visible, so that the telescope could be used to align the particle.

The threshold for vaporization was determined by attenuating the beam with known partially reflecting germanium mirrors until there was just sufficient intensity to visually observe a cloud of vaporized material.¹⁹ The ionization threshold was determined in the same manner except that the visual observation was an intense plasma ball along with severe beam attenuation. The threshold was defined as that value of laser beam intensity where the vaporization or the breakdown event occurred in one out of ten shots. Just as in conventional gas breakdown,¹¹ the threshold for the particle vaporization and for ionization were well-defined events and there was only a minor difference between the one out of ten threshold and the ten out of ten definition.

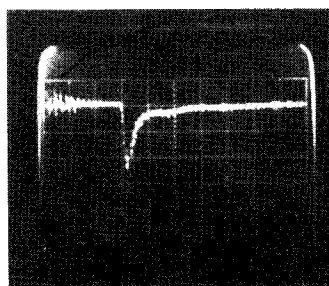
B. Experimental data

The vaporization and ionization thresholds of a number of materials were measured, including salt, carbon (graphite), aluminum, clay, and germanium. The particles were of one size and were sieved between 40 and 60 μ for a nominal size of 50- μ diameter, this 50- μ size being associated with the largest dimension of the particle. On viewing the particles through a microscope, it was observed that they had an irregular shape, but could be categorized as roughly elliptical, with the smaller dimension being roughly half that of the maximum particle dimension.

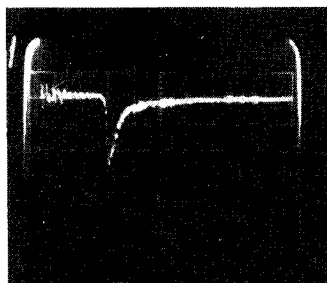
Experimental data for each particle included determining the vaporization threshold for two different laser

pulse shapes. The laser pulses used were as described previously. The ionization (i.e., plasma production) threshold was also measured and was observed visually as an intense flash which represented both ionization of the particle as well as ionization of a large volume of air. This observation was based on the fact that the observable plasma volume was a few mm in diameter and roughly 1 cm long and that this plasma volume could not have come just from the total atom content of the 50- μ -diam particle alone. Vaporization of the particles at lower intensities was observed as a cloud of material which appeared to expand uniformly from the focus and disappear from view. No light was observed from the particle in this case.

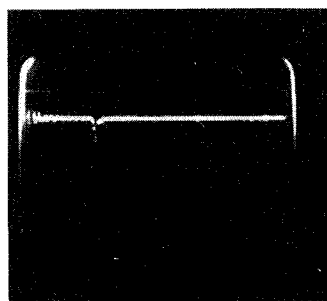
The difference between vaporization and ionization was very distinguishable visually because of the intense light emitted from the breakdown plasma. Also, the transmission through the focus of the incident laser light showed a significant difference between ionization



(a) 0.5 μ sec/div



(b) 0.5 μ sec/div



(c) 0.5 μ sec/div

FIG. 2. CO₂ laser pulses transmitted through vaporized carbon particles (50 μ particle diameter, 500 μ laser spot diameter). (a) Incident laser pulse; (b) transmitted pulse through vaporized carbon particle; (c) transmitted pulse through breakdown.

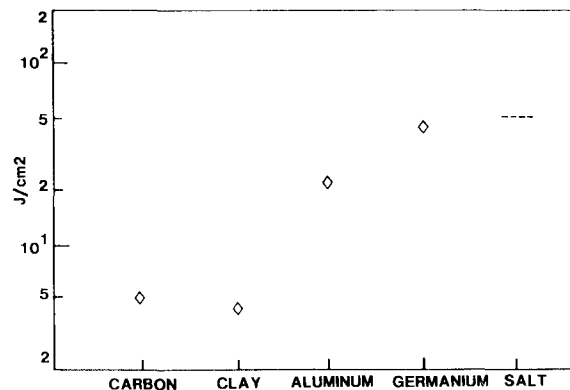


FIG. 3. Vaporization threshold flux for various materials (50- μ -diam particles).

and vaporization. A gold-doped germanium detector was used to monitor the laser radiation transmitted through the focus as depicted schematically in Fig. 1. The laser radiation was attenuated by a factor of 50 and focused onto the chip so that the detector recorded the total power transmitted through the focus. The transmission of the laser radiation through the focal region is shown in Fig. 2. Figure 2(a) shows the laser pulse time history when there was no particle at the focus, i.e., the undistorted laser pulse. This particular pulse had the 2- μ sec tail. When a particle was placed at the focus and vaporized (shattered) the transmitted pulse was not altered as is shown by the oscilloscope trace in Fig. 2(b). When the intensity of the laser was increased so that breakdown and plasma production were achieved, the laser pulse was severely attenuated as shown in Fig. 2(c). [The oscilloscope gain was adjusted such that in the absence of breakdown the signal was identical in amplitude to that in Fig. 2(a).] The attenuation was as high as 99% and persisted for at least 1 μ sec. The time required to go from maximum to minimum transmission was ~ 10 nsec.

If it is assumed that attenuation was first observed when the particle was ionized in its initial 50- μ diameter, then the vapor or plasma front must have expanded to the 500- μ diameter of the focal spot in this 10 nsec. This corresponds to a radial velocity of 2.5×10^6 cm/sec and can only be explained by the presence of a rapidly expanding radial wave. The velocity for a laser-supported detonation wave has been derived by Raizer¹ as

$$V = [2(\gamma^2 - 1)I/\rho_0]^{1/3}, \quad (1)$$

where γ is the specific heat ratio, I is the laser beam intensity in the beam, and ρ_0 is the initial density. For plasma production, the breakdown flux was 10^8 W/cm² and the density of the background air was 1.2×10^{-3} cm³. For these conditions the calculated expansion velocity is $\sim 10^6$ cm/sec which is in reasonable agreement with the expansion velocity estimated above based on the transmission cutoff time.

1. Vaporization threshold

The vaporization threshold of a number of different particle materials is shown in Fig. 3. Plotted in the

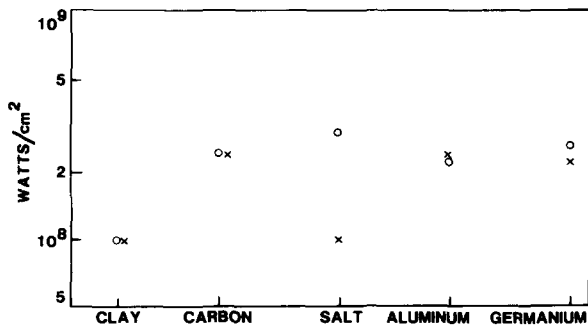


FIG. 4. Particle-induced breakdown threshold for various materials (50- μ -diam. particles); \circ —0.2 μ sec pulse—no tail; \times —0.2- μ sec pulse plus 2- μ sec tail.

figure is the minimum energy flux incident on the particle required to cause vaporization (shattering) for one out of ten shots. These data were obtained with both the short pulse and the pulse with the high-energy tail. No difference in threshold energy flux was discernible. The conclusion is that the threshold for vaporization is independent of the laser pulse duration and depends only on the energy flux and type of material, for laser pulses in the 0.1–1- μ sec range. The vaporization threshold of salt could not be determined since this threshold was greater than or equal to the ionization threshold, which is shown by the dashed line in Fig. 3.

The thresholds for vaporization of the 50- μ particles are surprisingly low. At the vaporization threshold, the total energy intercepted by the particle was in some cases less than that calculated for vaporization of the particle, based on its volume. For example, the heat of vaporization of aluminum is 6.7 kJ/g and, for the 50- μ -diam particle, $\sim 6 \times 10^{-3}$ J would be required for vaporization. The threshold measured is 20 J/cm² which represents only 2×10^{-3} J total energy incident on the particle. Even if the reflectivity of the particles is ignored, there does not appear to be sufficient energy to vaporize the particles. It thus appears that the particles were shattered into smaller pieces. These smaller particles would intercept more of the beam and could then be vaporized; implying a two-step process for vaporization.

2. Breakdown threshold

The ionization or breakdown thresholds of the particles in air were measured using the same type of particles as used in the vaporization measurements. The threshold intensities for breakdown are shown in Fig. 4. Again, the two different laser pulses were used and the data are marked accordingly. The threshold for ionization apparently depends on the peak intensity rather than on the total energy flux, since more energy for breakdown was required with the longer duration laser pulse. The most interesting feature of the data is that the thresholds for all of the materials are almost identical, being $1\text{--}2 \times 10^8$ W/cm² and are independent of particle material. It was thought that the thresholds may have been due to a water vapor film on the particles which would have made them appear to be the same. However, the particles were baked out in an oven to re-

move the moisture and no change in threshold was observed.

3. Particle size dependence

The particle size dependence of the threshold was examined using alumina particles (Al₂O₃). The size range was from 1- to 70- μ diameter and the threshold data are shown in Fig. 5. The numbers next to the data refer to the number of breakdowns observed out of ten shots. The threshold appears to be independent of particle size for the material and size range considered here. This is somewhat surprising in view of previously reported results by Lencioni¹³ which showed a size dependence for particles smaller than 10 μ . This discrepancy has not been resolved.

The particle sizes were determined by microphotographing a slide containing a sample of the particles. The large-size particles were spherical in shape and were within 10% of the specified size. The smaller particles (~ 8 μ) were irregular in shape and some variation in size was observed. The 1- μ particles had a tendency to adhere together and form clusters of 2 to 3 particles, which may have affected the measurement of the threshold.

4. Laser spot size dependence

The laser spot size in the previous experiments was fixed at 500- μ diameter. Since the laser interaction involved an expanding vapor, it was important to determine if the threshold depended on the relative size of the particle compared to the laser spot size. The focal diameter was varied by using different focal length lenses for the small diameters and by using spherical mirrors for the large diameters. The data for the breakdown threshold intensity of the various alumina particles as a function of laser beam diameter were obtained for a range of particles from 3- up to 50- μ diameter. The laser spot size was varied from 2.5×10^{-2} cm up to a maximum diameter of 0.15 cm. The data showed some scatter, with thresholds as low as 5×10^7 W/cm², and no systematic trend in the data was observed. It was therefore concluded that the breakdown threshold is independent of the laser beam diameter for these experimental conditions.

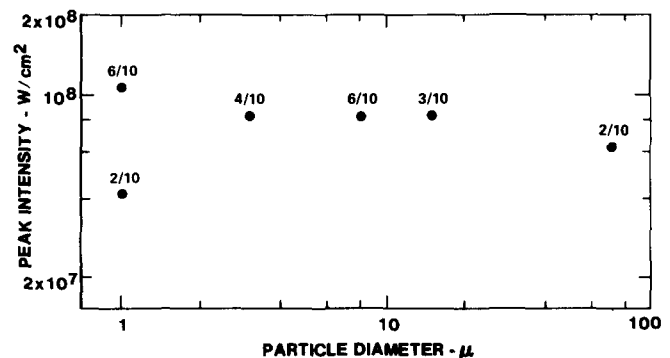


FIG. 5. Breakdown threshold vs particle diameter (alumina particles, 500- μ laser beam diameter, 0.2- μ sec pulse—no tail).

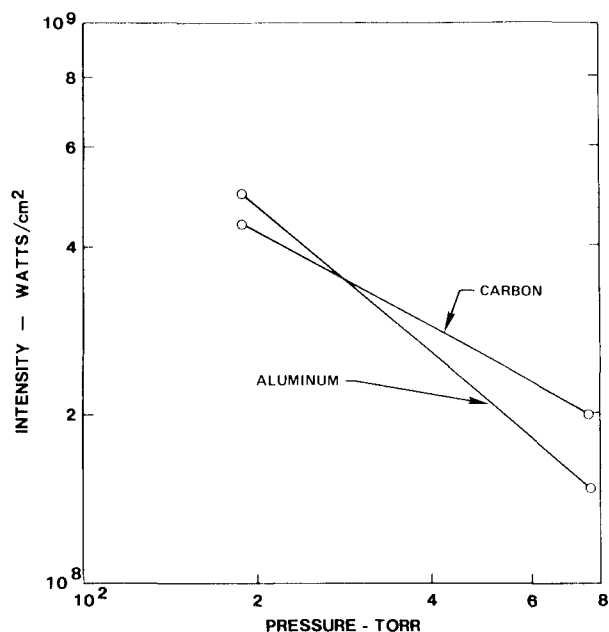


FIG. 6. Breakdown threshold vs background air pressure (50- μ -diam. particles).

5. Background gas pressure

The gas breakdown threshold of laboratory air had shown a pressure dependence.¹⁰ Since it was felt that the laboratory air threshold was controlled by aerosols, this pressure dependence could not be readily explained. One explanation was that the probability of finding an aerosol particle in the beam increased at high pressure.

In order to study this problem, a pressure-tight suspension cell was constructed. It was found that the suspension system could only be operated at pressures down to 170 Torr because of electrical breakdown between the suspension electrodes at low pressure. Also, it was not possible to charge the particles at lower pressures and so it was necessary to suspend the particles at atmospheric pressure and then reduce the pressure by slowly evacuating the chamber. The pressure dependence of the threshold of aluminum and carbon particles as a function of background air pressure is shown in Fig. 6. The aluminum particle breakdown had a slight dependence on background pressure while the carbon had a somewhat stronger pressure dependence. This pressure dependence is consistent with that observed for laboratory air.¹⁰ A possible explanation for this pressure dependence is that the reaction between the laser-heated vapor and the surrounding air occurred at a faster rate at higher pressures, thereby lowering the thresholds.

6. Particle plasma expansion

The expansion of the particle-induced breakdown plasma is of interest both in determining the mechanism causing the plasma production and also in determining the rate at which the laser beam is attenuated by the expanding plasma. An STL image convertor camera operating in the streak mode was used to examine the particle plasma expansion.

The streak photograph for a 50- μ -diam aluminum particle is shown in Fig. 7. A sketch of the lens and position of the focus is shown at the top of the figure and a streak photograph of the plasma luminosity growing toward the focusing lens is shown below the sketch. The initial position of the particle is also shown in the photograph. The lower photograph is an oscilloscope trace which shows the laser pulse (upper trace) and the ramping voltage pulse of the STL streak unit (lower trace) and shows the relationship of the laser intensity and the streak photograph. As closely as can be measured, the plasma luminosity is first recorded at the peak of the laser pulse and the expansion velocity is 7×10^5 cm/sec. This expansion velocity is in reasonable agreement with the radiation-supported blast wave theory of Raizer given in Eq. (1).

7. Schlieren studies

The schlieren system shown in Fig. 8 was used to investigate the interaction of the laser radiation with the single solid particle and to look at the density gradients induced in the surrounding air. The schlieren system was set up looking through the suspension cube and transverse to the direction of the laser propagation. The schlieren spark source emitted a light pulse with a 50-nsec half-width, allowing the observation of high Mach number shock waves in air; and the viewing optics provided a 20 \times magnification, allowing the observation of

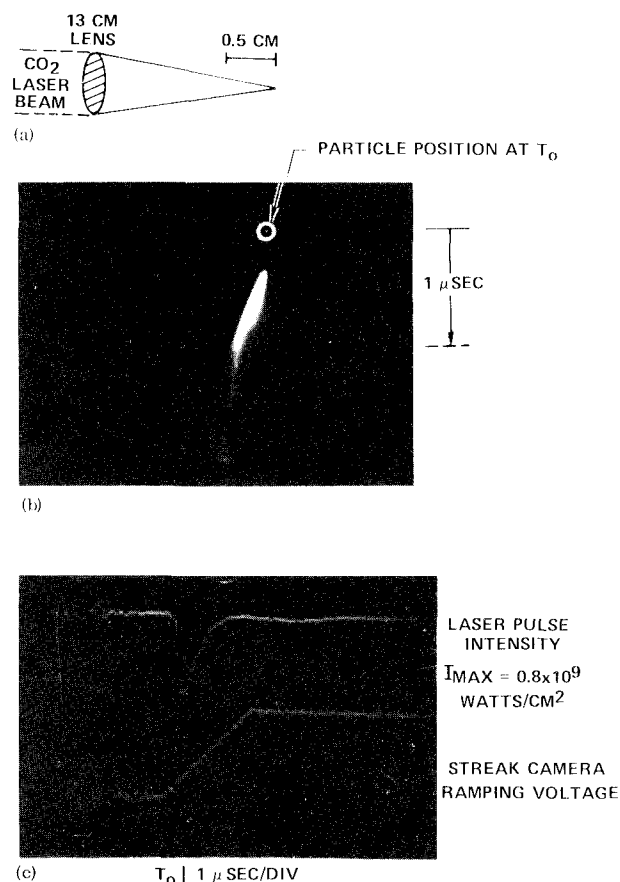


FIG. 7. Streak photograph of particle-induced gas breakdown (50- μ -diam. aluminum particle).

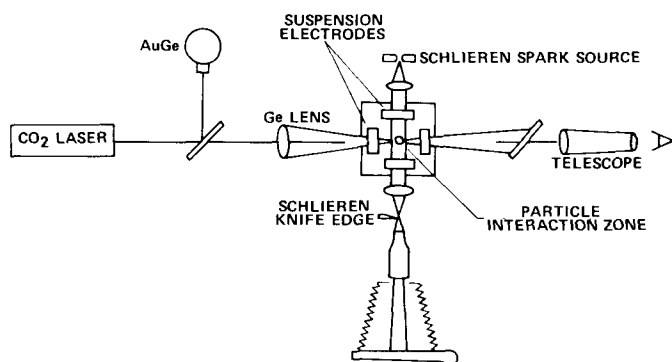


FIG. 8. Diagram of particle suspension apparatus and schlieren system.

particles down to $5\ \mu$ in diameter. Because of spatial and temporal resolution limitations, the system was not intended for use during the laser pulse; i.e., attempts were not made to photograph the particle during the time in which it was actually being irradiated by the laser pulse. Instead the system was used primarily to study the following two questions: (i) Whether the particle could be vaporized sufficiently to generate a shock wave in air, without causing actual breakdown and (ii) whether the particle was vaporized first and then ionized, causing breakdown; or was only partially vaporized when breakdown occurred.

A typical set of schlieren photographs is shown in Fig. 9. In these pictures, the laser pulse consisted of a 200-nsec half-width spike with no tail, and the schlieren spark source was fired 500 nsec after the peak of the laser pulse. The particles were $50\text{-}\mu$ -diam carbon suspended in STP air, and the laser focal diameter was $500\ \mu$. The first picture shows that a vapor-driven shock wave was generated at the particle at a flux below that required for breakdown. The second photograph corresponds to an intensity very close to threshold. It should be noted that the luminosity due to the breakdown plasma is time integrated (there was no shutter on the schlieren camera) whereas the shock image corresponds to a given instant of time. The striations in the breakdown plasma may be due to self-mode locking of the TEA laser. The final photograph in Fig. 9 is for an intensity well above threshold and clearly shows that the breakdown was initiated at the front surface of the particle, leaving the particle more or less intact. It appears that the breakdown region expanded to fill the laser focal volume, and then propagated back toward the laser.

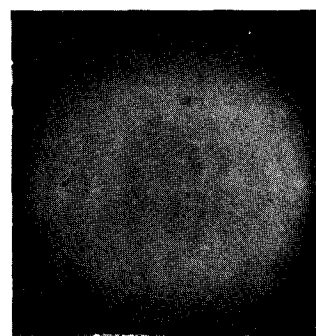
All of the data taken in this series of tests were for the optically thick particle case (i.e., $x = 2a/\lambda > 1$, where a is the particle radius), and as expected, the results indicate that breakdown occurred at the front surface of the particle. While insufficient tests were carried out to determine whether shock heating of the air or direct surface heating initiated breakdown, one can conclude that breakdown occurred prior to complete vaporization of the particle.

III. DISCUSSION

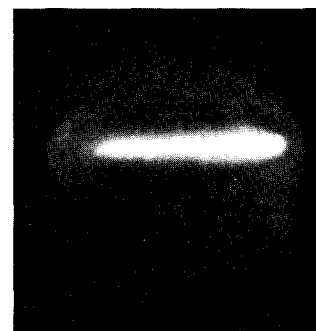
In order to understand the effects of particulate

matter on the breakdown threshold, it is necessary to look at three phases in the laser-particle interaction: (i) the laser energy absorption process at the surface of the particle or in the particle volume; (ii) the particle vaporization kinetics; and (iii) the interaction of the vapor with the ambient air. In general, these processes are coupled together, but to a first approximation, they can be analyzed separately.

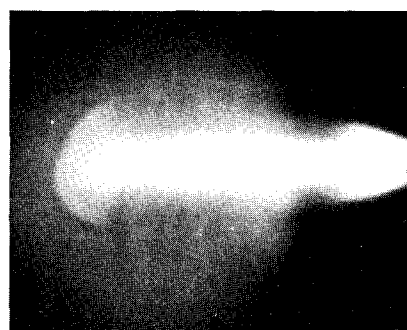
There appear to be two mechanisms whereby a particle can reduce the threshold below that associated with the clean gas. With the first mechanism, the particle can absorb the laser energy directly, producing a vapor which absorbs the laser radiation only weakly, but which drives a hydrodynamic shock wave into the surrounding gas. For sufficiently strong shock waves, the air would



(a)



(b)



(c)

FIG. 9. Pulsed laser-particle heating ($50\text{-}\mu$ carbon particles, $500\text{-}\mu$ beam diameter). (a) Peak intensity $= 6.0 \times 10^7\ \text{W/cm}^2$. (b) Peak intensity $= 1.0 \times 10^8\ \text{W/cm}^2$. (c) Peak intensity $= 2.4 \times 10^8\ \text{W/cm}^2$.

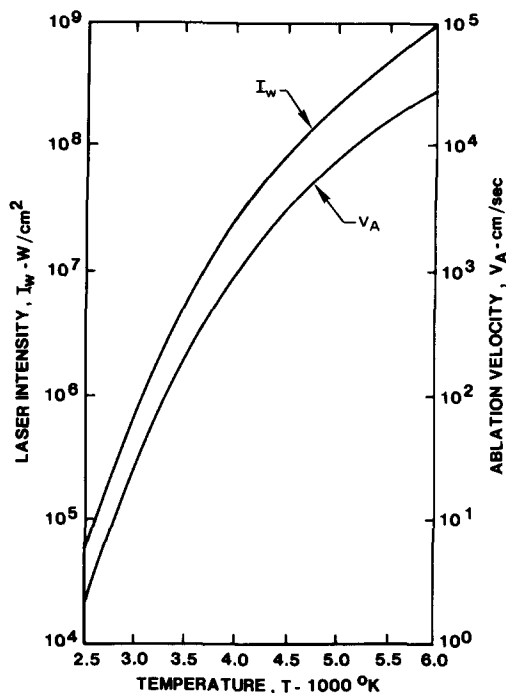


FIG. 10. Surface temperature and ablation velocity vs incident laser intensity.

be ionized to a high enough level to initiate gas breakdown via cascade ionization. The second possible mechanism would not involve shock heating of the air, but would lead to breakdown through the laser-surface interaction itself. If the temperature at the surface reached a high enough value, a significant number of electrons would be produced, either by thermionic emission or by thermal ionization, and cascade breakdown would propagate into the surrounding vapor and subsequently into the surrounding air.

Most of the previous studies of laser-solid interactions have concentrated on the laser-surface interaction²⁰⁻²³ and have assumed that the vapor expands into vacuum. The details of the absorption process were not considered, but were accounted for instead by utilizing the experimentally observed fact that the absorption length for strongly absorbing materials is very small (10^{-5} – 10^{-4} cm). These studies showed that for laser intensities greater than 10^6 W/cm², thermal conduction within the material is negligible, and that for laser intensities less than 10^9 W/cm², absorption of the laser radiation by the vapor phase is negligible. Since measurements indicate that the breakdown threshold for aerosol-laden atmospheric pressure air is in the above range, the above analyses are relevant to the aerosol breakdown problem. Afanasev *et al.*²⁴ and Triplett and Boni²⁵ have considered the interaction of the expanding vapor with an ambient gas and have shown that if the gas density and pressure are small compared to those of the vapor, the expansion is similar to that into vacuum, and the vapor acts as a piston, driving a shock wave into the ambient air. As mentioned above, one possible breakdown mechanism is for this shock wave to be strong enough to generate ionization in the gas.

An approximate analysis of the vapor-driven shock

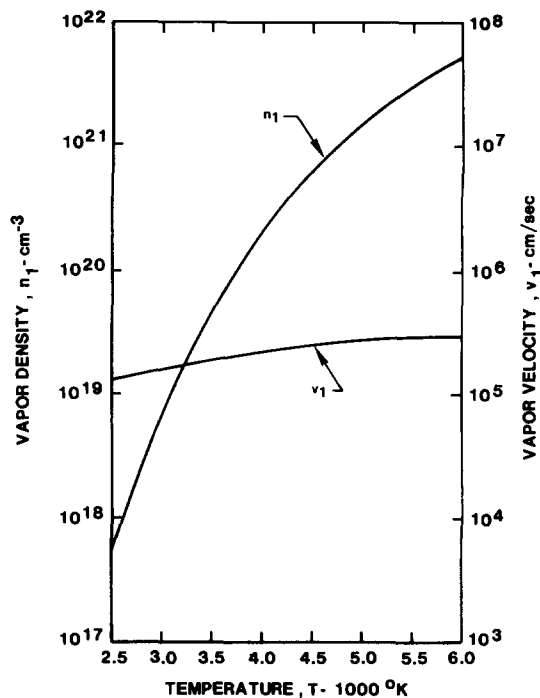


FIG. 11. Vapor density and vapor velocity vs surface temperature.

wave problem can be carried out for quartz using the results of Chang *et al.*²³ Their model, which should be applicable to optically thick particles, has been used to calculate the vapor temperature and ablation velocity as a function of the laser intensity and the results are shown in Fig. 10. Using the equation of state in Ref. 23, the density of the vapor can also be obtained as a function of the vapor temperature as well as the vapor velocity

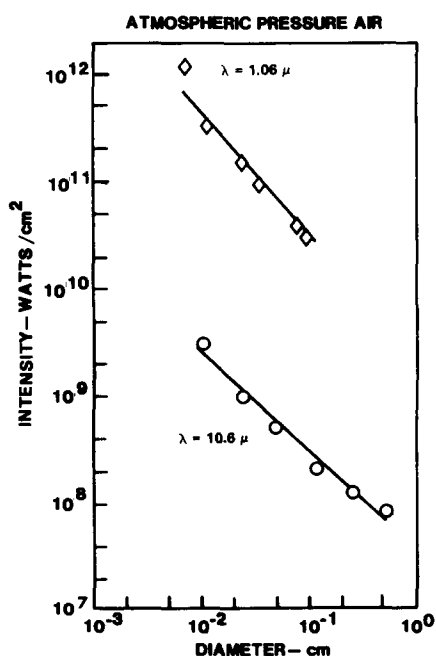


FIG. 12. Aerosol-induced breakdown threshold vs beam diameter for 10.6-μ wavelength and 1.06-μ wavelength.

as shown in Fig. 11. For laser intensities in the range 10^6 – 10^8 W/cm², the results show that the shock-heated air reaches a temperature of 5000°K, which would correspond to an ionization fraction in air of 10^{-4} , i.e., high enough to initiate breakdown. However, as seen from Figs. 10 and 11, the vapor expansion velocity (and thus the vapor-driven shock strength) are relatively weak functions of the incident intensity. On the other hand, in the experiments, the particles showed a very sharp threshold for breakdown. Based on this comparison, it appears that the vapor-driven shock mechanism is not the mechanism causing breakdown.

While the shock heating above cannot account for the breakdown threshold, the above results do indicate that high temperatures and high densities can be produced in the region near the surface of the particle, even for intensities significantly below those for clean air breakdown. These conditions could then produce the initial electrons for cascade ionization and breakdown in the vapor/air mixture near the particle. In addition, since the inverse bremsstrahlung heating rate would be higher in the high-density vapor than in the surrounding air, the cascade processes would be faster, further lowering the threshold. Also, for sufficiently high temperatures a large number of ions would be formed, and the electron-ion collision processes would add to the cascade process. The above conclusions, which are similar to those reached by Lencioni,²⁶ require detailed analytical modeling for further verification.

One important aspect of the breakdown process is its wavelength dependence. We can use previous data obtained at 1.06 μ and compare them with the 10.6- μ data. As discussed in Sec. I, the lab-air threshold decreased with increasing focal volume size and this was apparently caused by particulate matter present in the air. Thus the threshold of lab air in large focal spots is in reality the threshold of particles, rather than of the air. From Ref. 2, the 1.06- μ data for lab air have been compared with the 10.6- μ data from Ref. 11, and the results are shown in Fig. 12.²⁷ These curves show that the threshold for lab air (and therefore of aerosols) scales as λ^{-2} , i.e., the threshold with neodymium laser radiation is a factor of 100 larger than that observed at 10.6 μ . This comparison indicates that while the aerosol breakdown is initiated at the particle, it is controlled partly by the cascade ionization in the vapor/air mixture and therefore has the wavelength dependence characteristic of a cascade process. This agrees with the recent experimental results reported by Lencioni²⁶ where he measured thresholds of carbon particles in air with 1.06- μ radiation and compared these data with 10.6- μ wavelength data.

IV. CONCLUSIONS

The data presented above show that an important limitation for high-power laser propagation is that associated with aerosol-induced breakdown. For the particle sizes and materials considered in the present study, the threshold for breakdown was in the range 5×10^7 – 2×10^8 W/cm² and tended to be independent of particle diameter and particle material. In the single-particle experiments of the present study, no dependence on

focal volume size was observed, indicating that the focal volume dependence observed in propagation through ordinary air is due to the increased probability of finding particles in large focal volumes. While the above threshold is significantly below that for clean air, and thus represents a much greater limitation for atmospheric propagation, it should be noted that with aerosol-induced breakdown there is a finite time required for the plasma to fill the laser beam and to limit the laser power transmitted. This effect has been considered by Lencioni²⁸ and also by Nielsen,²⁹ who show that the time required for plasma shielding with large beams and long paths can be a significant effect.

While the physics of the aerosol-induced breakdown process is not well understood, it appears that the most likely mechanism is the generation of electrons at the surface of the heated particle. These electrons then multiply in a cascade process in the high-density vapor at the particle surface and subsequently in the air surrounding the particle. These cascade processes give the breakdown threshold the wavelength and pressure dependences similar to those predicted by rf heating.

ACKNOWLEDGMENTS

The authors wish to thank L. J. Muldrew and R. E. Lee for their technical assistance in carrying out the experiments. This research was supported in part by the Office of Naval Research.

- ¹Yu. P. Raizer, *Sov. Phys.-Usp.*, **8**, 650 (1966).
- ²A. F. Haught, R. G. Meyerand, Jr., and D. C. Smith, in *Physics of Quantum Electronics*, edited by P. L. Kelley, B. Lax, and P. E. Tannerwald (McGraw-Hill, New York, 1966), p. 509.
- ³R. G. Tomlinson, E. K. Damon, and H. T. Buscher, in Ref. 1, p. 520.
- ⁴S. C. Brown, *Handbuch der Physik* (Springer Verlag, Berlin, 1956), pp. 531–574.
- ⁵In microwave breakdown, because of the low pressures and continuous microwave sources, diffusion-dominated breakdown is often observed. This threshold exhibits a (diameter)⁻² dependence. However for pulsed lasers and pressures of atmospheric and above, the time required for diffusion is generally long compared to the laser pulse duration and can be ignored.
- ⁶D. C. Smith and A. F. Haught, *Phys. Rev. Lett.*, **16**, 1085 (1966).
- ⁷B. F. Mul'chenko, and Yu. P. Raizer, *Sov. Phys.-JETP*, **33**, 349 (1971).
- ⁸N. A. Generalov, V. P. Zimakov, G. I. Kozlov, V. A. Masyukov, and Yu. P. Raizer, *JETP Lett.*, **11**, 228 (1970); D. C. Smith, *J. Appl. Phys.*, **41**, 4501 (1970).
- ⁹For shorter wavelengths ($\lambda < 8000$ Å) the threshold decreased with decreasing wavelength; see, for example, H. T. Buscher, R. G. Tomlinson, and E. K. Damon, *Phys. Rev. Lett.*, **15**, 847 (1965); A. J. Alcock, C. DeMichelis, and M. C. Richardson, *Appl. Phys. Lett.*, **15**, 72 (1969).
- ¹⁰D. C. Smith, *Appl. Phys. Lett.*, **19**, 405 (1971).
- ¹¹D. C. Smith and P. J. Berger (unpublished).
- ¹²G. H. Canavan and P. E. Nielsen, *Appl. Phys. Lett.*, **22**, 409 (1973).
- ¹³D. E. Lencioni, *Appl. Phys. Lett.*, **23**, 12 (1973).
- ¹⁴D. C. Smith, P. J. Berger, R. T. Brown, and M. C. Fowler (unpublished).
- ¹⁵R. T. Brown and D. C. Smith, *Appl. Phys. Lett.*, **22**, 245 (1973).

- ¹⁶D.C. Smith and A.J. DeMaria, J. Appl. Phys. **41**, 5212 (1970).
- ¹⁷R.F. Wuerber, H.M. Goldenberg, and R.V. Langmuir, J. Appl. Phys. **30**, 441 (1959).
- ¹⁸A.F. Haught, and D.H. Polk, Phys. Fluids **9**, 2047 (1966).
- ¹⁹Because of the high index of refraction of germanium and slight wedge associated with some of the mirrors, it was found that some error in positioning of the focus could occur and it was necessary to take care in aligning the laser beam with the attenuators in place.
- ²⁰Yu. V. Afanasev and O.N. Krokhin, Sov. Phys.-JETP **25**, 639 (1967).
- ²¹S.I. Anisimov, A.M. Bonch-Bruevich, M.A. El'yashevich, Ya A. Imus, N.A. Pavlenko, and G.S. Romanov, Sov. Phys.-Tech. Phys. **11**, 945 (1967).
- ²²S.I. Anisimov, Sov. Phys.-JETP **27**, 182 (1968).
- ²³D.B. Chang, J.E. Drummond, and R.B. Hall, J. Appl. Phys. **41**, 4851 (1970).
- ²⁴Yu. V. Afanasev, N.G. Basov, O.N. Krokhin, N.Y. Morachevskii, and G.V. Skilizkov, Sov. Phys.-Tech. Phys. **14**, 669 (1969).
- ²⁵J.R. Triplett and A.A. Boni, AFWL-TR-72-102, 1972 (unpublished).
- ²⁶D.E. Lencioni, Appl. Phys. Lett. **25**, 15 (1974).
- ²⁷In order to obtain this comparison for the same focal spot diameters, it was necessary to extrapolate the 1.06- μ data from the 16-atm background pressure to 1 atm using the experimentally observed $p^{-1/2}$ dependence.
- ²⁸D.E. Lencioni (private communication).
- ²⁹P.E. Nielsen (private communication).